



Heriot-Watt University
Research Gateway

Full-Asynchronous Gigabit-Symmetric DPSK Downstream and OOK Upstream OCDMA-PON with Source-Free ONUs Employing All-Optical Self-Clocked Time Gate

Citation for published version:

Dai, B, Shimizu, S, Wang, X & Wada, N 2012, 'Full-Asynchronous Gigabit-Symmetric DPSK Downstream and OOK Upstream OCDMA-PON with Source-Free ONUs Employing All-Optical Self-Clocked Time Gate', *Optics Express*, vol. 20, no. 6, pp. B21-B31. <https://doi.org/10.1364/OE.20.000B21>

Digital Object Identifier (DOI):

[10.1364/OE.20.000B21](https://doi.org/10.1364/OE.20.000B21)

Link:

[Link to publication record in Heriot-Watt Research Portal](#)

Document Version:

Publisher's PDF, also known as Version of record

Published In:

Optics Express

General rights

Copyright for the publications made accessible via Heriot-Watt Research Portal is retained by the author(s) and / or other copyright owners and it is a condition of accessing these publications that users recognise and abide by the legal requirements associated with these rights.

Take down policy

Heriot-Watt University has made every reasonable effort to ensure that the content in Heriot-Watt Research Portal complies with UK legislation. If you believe that the public display of this file breaches copyright please contact open.access@hw.ac.uk providing details, and we will remove access to the work immediately and investigate your claim.

Full-asynchronous gigabit-symmetric DPSK downstream and OOK upstream OCDMA-PON with source-free ONUs employing all-optical self-clocked time gate

Bo Dai,¹ Satoshi Shimizu,² Xu Wang,^{1,*} and Naoya Wada²

¹*School of Engineering and Physical Sciences, Heriot-Watt University, Edinburgh, EH14 4AS, UK*

²*Photonic Network Research Institute, National Institute of Information and Communications Technology, Tokyo, 184-8795, Japan*

**x.wang@hw.ac.uk*

Abstract: We propose an asynchronous gigabit-symmetric optical code division multiplexing access passive optical network (OCDMA-PON) in which optical network units (ONUs) are source-free. In the experiment, we demonstrate a duplex OCDMA system with a 50 km 10 Gbit/s/user 4-user DPSK-OCDMA downlink and a 50 km 10 Gbit/s/user 4-user OOK-OCDMA uplink and error-free duplex transmissions are achieved. Besides, we investigate an all-optical self-clocked time gate, which is used for the signal regeneration of decoded signals and ensures asynchronization in the up/downstream transmissions. Furthermore, we evaluate the power budget of the proposed duplex transmission.

©2012 Optical Society of America

OCIS codes: (060.0060) Fiber optics and optical communications; (060.4250) Networks; (060.4080) Modulation; (070.4340) Nonlinear optical signal processing.

References and links

1. K. Kitayama, X. Wang, and N. Wada, "OCDMA over WDM PON—solution path to gigabit-symmetric FTTH," *J. Lightwave Technol.* **24**(4), 1654–1662 (2006).
2. Z. A. El-Sahn, B. J. Shastri, Z. Ming, N. Kheder, D. V. Plant, and L. A. Rusch, "Experimental demonstration of a SAC-OCDMA PON with burst-mode reception: local versus centralized sources," *J. Lightwave Technol.* **26**(10), 1192–1203 (2008).
3. N. Kataoka, N. Wada, X. Wang, G. Cincotti, A. Sakamoto, Y. Terada, T. Miyazaki, and K. Kitayama, "Field trial of duplex, 10 Gbps x 8-user DPSK-OCDMA system using a single 16x16 multi-port encoder/decoder and 16-level phase-shifted SSFBG encoder/decoders," *J. Lightwave Technol.* **27**(3), 299–305 (2009).
4. J. Liu, D. Zeng, C. Guo, L. Xu, and S. He, "OCDMA PON supporting ONU inter-networking based on gain-switched Fabry-Pérot lasers with external dual-wavelength injection," *Opt. Express* **18**(22), 22982–22987 (2010).
5. P. J. Urban, B. Huiszoon, R. Roy, M. M. de Laat, F. M. Huijskens, E. J. Klein, G. D. Khoe, A. M. J. Koonen, and H. de Waardt, "High-bit-rate dynamically reconfigurable WDM-TDM access network," *J. Opt. Commun. Netw.* **1**(2), A143–A159 (2009).
6. G. Cincotti, N. Kataoka, N. Wada, X. Wang, T. Miyazaki, and K. Kitayama, "Demonstration of asynchronous, 10Gbps OCDMA PON system with colorless and sourceless ONUs," in 35th European Conference and Exhibition on Optical Communication (ECOC 2009), Vienna, Austria, paper 6.5.7 (2009).
7. W. Hung, C. K. Chan, L. K. Chen, and F. Tong, "An optical network unit for WDM access networks with downstream DPSK and upstream remodulated OOK data using injection-locked FP laser," *IEEE Photon. Technol. Lett.* **15**(10), 1476–1478 (2003).
8. C. W. Chow, "Wavelength remodulation using DPSK down-and-upstream with high extinction ratio for 10-Gb/s DWDM-passive optical networks," *IEEE Photon. Technol. Lett.* **20**(1), 12–14 (2008).
9. J. Yu, M. F. Huang, D. Qian, L. Chen, and G. K. Chang, "Centralized lightwave WDM-PON employing 16-QAM intensity modulated OFDM downstream and OOK modulated upstream signals," *IEEE Photon. Technol. Lett.* **20**(18), 1545–1547 (2008).
10. B. Dai, S. Shimizu, X. Wang, and N. Wada, "Full-asynchronous gigabit-symmetric OCDMA-PON with source-free ONUs based on DPSK downstream and remodulated OOK upstream links," in 38th European Conference and Exhibition on Optical Communication (ECOC 2012), Amsterdam, the Netherlands, paper Mo.1.B.5 (2012).
11. P. C. Teh, P. Petropoulos, M. Ibsen, and D. J. Richardson, "A comparative study of the performance of seven and 63-chip optical code-division multiple-access encoders and decoders based on superstructured fiber Bragg gratings," *J. Lightwave Technol.* **19**(9), 1352–1365 (2001).

12. B. Dai, Z. Gao, X. Wang, N. Kataoka, and N. Wada, "Performance comparison of $0/\pi$ - and $\pm \pi/2$ -phase-shifted superstructured Fiber Bragg grating en/decoder," *Opt. Express* **19**(13), 12248–12260 (2011).
13. G. Cincotti, N. Wada, and K. Kitayama, "Characterization of a full encoder/decoder in the AWG configuration for code-based photonic routers — part I: modeling and design," *J. Lightwave Technol.* **24**(1), 103–112 (2006).
14. A. Agarwal, P. Toliver, R. Menendez, S. Etamad, J. Jackel, J. Young, T. Banwell, B. E. Little, S. T. Chu, W. Chen, W. Chen, J. Hryniewicz, F. Johnson, D. Gill, O. King, R. Davidson, K. Donovan, and P. J. Delfyett, "Fully programmable ring-resonator-based integrated photonic circuit for phase coherent applications," *J. Lightwave Technol.* **24**(1), 77–87 (2006).
15. X. Wang and Z. Gao, "Novel reconfigurable 2-dimensional coherent optical en/decoder based on coupled micro-ring reflector," *IEEE Photon. Technol. Lett.* **23**(9), 591–593 (2011).
16. I. Widjaja, "Performance analysis of burst admission-control protocols," *IEE Proc. Commun.* **142**(1), 7–14 (1995).
17. K. E. Stubkjaer, "Semiconductor optical amplifier-based all-optical gates for high-speed optical processing," *IEEE J. Sel. Top. Quantum Electron.* **6**(6), 1428–1435 (2000).
18. V. J. Hernandez, W. Cong, J. Hu, C. Yang, N. K. Fontaine, R. P. Scott, Z. Ding, B. H. Kolner, J. P. Heritage, and S. J. B. Yoo, "A 320-Gb/s capacity (32-user \times 10 Gb/s) SPECTS O-CDMA network testbed with enhanced spectral efficiency through forward error correction," *J. Lightwave Technol.* **25**(1), 79–86 (2007).
19. K. L. Deng, I. Glesk, K. I. Kang, and P. R. Prucnal, "Unbalanced TOAD for optical data and clock separation in self-clocked transparent OTDM networks," *IEEE Photon. Technol. Lett.* **9**(6), 830–832 (1997).
20. N. Wada, H. Sotobayashi, and K. Kitayama, "Error-free 100km transmission at 10Gbit/s in optical code division multiplexing system using BPSK picosecond-pulse code sequence with novel time-gating detection," *Electron. Lett.* **35**(10), 833–834 (1999).
21. X. Wang, T. Hamanaka, N. Wada, and K. Kitayama, "Dispersion-flattened-fiber based optical threshold for multiple-access-interference suppression in OCDMA system," *Opt. Express* **13**(14), 5499–5505 (2005).
22. R. Elschner, C.-A. Bunge, and K. Petermann, "System impact of cascaded all-optical wavelength conversion of DQPSK signals in transparent optical networks," *J. Netw.* **5**, 219–224 (2010).
23. Y. Ma, Y. Qian, G. Peng, X. Zhou, X. Wang, J. Yu, Y. Luo, X. Yan, and F. Effenberger, "Demonstration of a 40Gb/s time and wavelength division multiplexed passive optical network prototype system," in *Optical Fiber Communication Conference (OFC)*, Los Angeles, California, paper PDP5D (2012).
24. X. Wang, K. Matsushima, A. Nishiki, N. Wada, and K. Kitayama, "High reflectivity superstructured FBG for coherent optical code generation and recognition," *Opt. Express* **12**(22), 5457–5468 (2004).

1. Introduction

In the passive optical networks (PON), downstreams are broadcast to all end users, so it is necessary to encrypt the transmitted signals to guarantee information privacy and prevent eavesdropping. Optical code-division multiplexing (OCDM) techniques provide an attractive feature on security enhancement to address this information privacy issue. Besides, OCDM techniques have various advantages including fully asynchronous transmission, high network flexibility and protocol transparency. Therefore, OCDM techniques can be applied for new-generation PONs, where secure gigabit-symmetric transmissions are required to meet the needs of future bidirectional high data-rate applications such as telediagnosis services and video conference services [1]. Recently, many researches have proposed and demonstrated OCDM techniques in the PON. El-Sahn et al. demonstrated an architecture consisting of a standalone uplink burst-mode receiver in a 622 Mbit/s/user 7-user incoherent spectral amplitude coded (SAC) OCDMA-PON with local sources or centralized sources [2]. A full-asynchronous 10 Gigabit Ethernet (GbE) interface OCDMA prototype architecture was demonstrated in a field trial of duplex 10 Gbit/s/user 8-user differential phase-shift keying (DPSK)-OCDMA system over 100 km by using hybrid multi-port arrayed waveguide grating (AWG) and superstructured fiber Bragg grating (SSFBG) encoders/decoders [3]. In addition, an OCDMA-PON with optical network units (ONUs) inter-networking was demonstrated using gain-switched Fabry-Pérot (FP) lasers with external dual-wavelength injection [4]. In [5, 6], OCDMA-PONs with source-free ONUs were proposed and realized in the incoherent and coherent OCDMA-PON by sending un-modulated and non-coded optical carrier from the central office to ONUs for upstream transmission.

In the PON, an ONU processes the conversion between optical signals and electrical signals at a user's premise. The complexity of ONUs should be mitigated to reduce the cost of end users. To simplify the structure of ONUs, several remodulation schemes have been proposed in the different PONs. A 2.5 Gbit/s on-off keying (OOK) upstream transmitter was proposed for remodulation in a wavelength division multiplexing (WDM)-PON by directly modulating an FP laser which was injection-locked by a 10 Gbit/s DPSK downstream signal

[7]. A wavelength remodulation scheme using DPSK formats in both downstream and remodulated upstream was demonstrated in a 10 Gbit/s DWDM-PON [8]. In [9], a centralized lightwave remodulation scheme which employed a 10 Gbit/s quadrature amplitude modulation (16-QAM) downstream and a remodulated 2.5 Gbit/s OOK upstream was proposed in an orthogonal frequency-division multiplexing (OFDM)-WDM-PON.

In this paper, we extend our recent work [10] to show a full picture of an asynchronous gigabit-symmetric DPSK-downstream and remodulated OOK-upstream OCDMA-PON. The paper is organized as follows. In Section 2, we describe the proposed OCDMA-PON architecture. Then, we introduce an all-optical self-clocked time gate in Section 3, which is a key component used in the ONUs for signal regeneration. In Section 4, we show our experimental demonstration and results. Next, in Section 5, we investigate the performance improvement by employing self-clocked time gate and evaluate the power budget of the duplex transmission. Finally, the paper is summarized in Section 6.

2. OCDMA-PON architecture

The proposed OCDMA-PON architecture is shown in Fig. 1. In the optical line termination (OLT) which serves as a service provider and processes the coordination of multiplexing, a broadband light source, e.g. a mode-locked laser diode (MLLD), is used to generate a train of short optical pulses. This pulse train is split into N branches (where N is the number of total users) and modulated by N phase modulators (PM). The phase modulation can be any advanced M-ary (D)PSK formats. Then, the modulated signals are encoded by encoders which could be SSFBG encoders [11, 12], multi-port AWG encoders [13], or micro-ring-reflector (MRR) based encoders [14, 15]. The encoded signals are low-intensity noise-like signals and are multiplexed by a power coupler for downlink transmission.

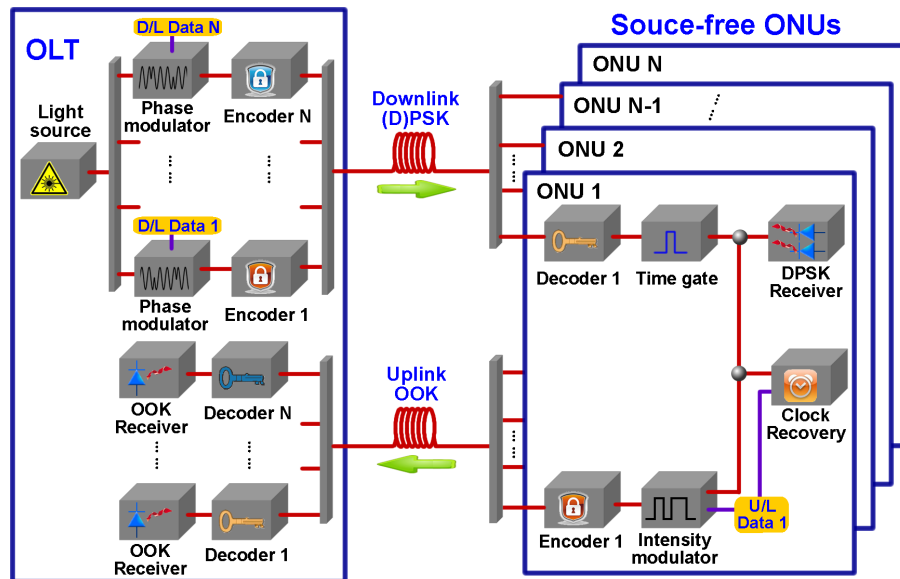


Fig. 1. Diagram of the proposed OCDMA-PON architecture.

At the ONU side, the multiplexed encoded signals are split into N branches by a power splitter. In each ONU, a corresponding decoder is used for decoding the signal. Correctly decoded signals are recovered into high-intensity peak pulses while incorrectly decoded signals remain low intensity, which produce multiple-access interference (MAI). The following signal regeneration process, where a time gate or a phase-preserving thresholder can be used, is to extract the correctly decoded signals and to suppress the MAIs. Then, the signals are separated into two branches. In one branch, the signal is demodulated and detected in the receiver. In the other branch, the signal is used for the upstream transmission. This

upstream signal is further split into two. One is input into a clock-recovery device for clock extraction and the other is input into an intensity modulator (IM) whose input electrical data are synchronized by the extracted clock. The intensity-modulated signal is encoded and multiplexed with the encoded signals from other ONUs for the transmission to the OLT, where the upstream signal is split into N branches for decoding and detection.

An efficient network control is needed for this OCDMA-PON. Since downstream and upstream transmissions use the same optical carrier, the light source in the OLT generates the optical carrier once it requires data transmissions between the OLT and ONUs. The status of PM and IM shifts between operating and idle mode depending on whether there is data to transmit. Thus, upstream transmissions are not affected even if there is no downlink data to transmit.

In the proposed OCDMA-PON, the data rate in the uplink can be as high as that in the downlink, because the upstream modulation is a direct intensity modulation of the downstream signal and the coding mechanisms for both downlink and uplink are same. Thus, gigabit-symmetric transmissions can be achieved. Besides the contribution to the high data rate of uplink, the remodulation scheme can simplify the ONUs by omitting light sources, which agrees the intention of the network design. In this network, synchronization is only needed during the remodulation in the ONUs locally and is not necessary for the duplex transmission. Therefore, the proposed OCDMA-PON can provide full-asynchronous transmission for both downlink and uplink and use the Tell-and-Go (TaG) protocol [16]. Comparing to other source-free-ONU OCDMA-PONs [5, 6], the proposed scheme does not require additional non-modulated and non-coded optical carriers from OLT for upstream transmission.

3. All-optical self-locked time gate

Optical time gates, widely used for wavelength conversion, optical signal regeneration, and demultiplexing, are essential devices in the optical communication networks [17]. Besides, time gates are also widely used in the optical code based technologies for signal extraction and multiple-access interference (MAI) suppression [18]. However, in a time gate, a synchronous clock signal is needed to extract a target signal from a data stream, which increases the complexity of systems and obliges systems to abandon the advantage of asynchronous transmission. To avoid using additional clock signal, self-locked time gates have been proposed, where a clock signal can be obtained and used to extract a target signal from an original data stream [19, 20].

In the ONUs of the proposed OCDMA-PON, we use an all-optical self-locked time gate, which simplifies the system in the ONUs and ensures asynchronous up/downlink transmission, for signal extraction and MAI suppression. The proposed self-locked time gate consists of two stages, as shown in Fig. 2. The first stage is to obtain a clock signal from an original signal, which consists of data and MAIs, and the second stage is to extract the data from the original signal.

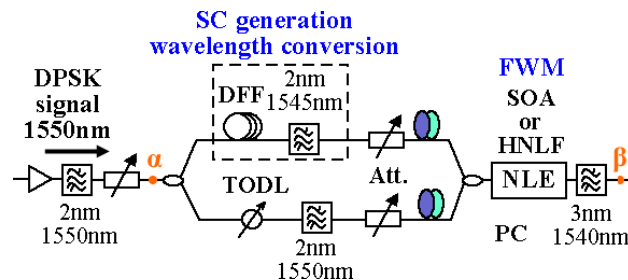


Fig. 2. Setup of the self-locked time gate.

In the first stage, an input signal is separated into two branches. In the upper branch, a supercontinuum (SC) based threshold, which consists of a dispersion flattened fiber (DFF)

and a bandpass filter (BPF), is used to generate a clock signal. In the DFF, only high-intensity pulses can generate SC, while low-intensity noises cannot generate SC. The following filter centered at another wavelength only allows the generated SC pass through. As a result, a train of high-intensity pulses with the same repetition rate of the data, i.e. a clock signal, is obtained. The SC based threshold is widely used for MAI suppression in the OOK-OCDMA system [21], but it is not suitable for DPSK systems, because the phase information cannot be preserved during the SC generation [22]. Thus, this technique is used for the extraction of clock signal instead of the reshaping of DPSK signals. The signal in the lower branch is adjusted by a tunable optical delay line (TODL) to ensure that the pulses are temporally overlapped with the pulses in the clock signal after a 3-dB coupler.

In the second stage, the coupled signals are injected into a nonlinear element (NLE) for four-wave mixing (FWM), which is a time gating process. In the FWM process, a phase-conjugate replica of the target signal is generated. A following filter is to filter out the generated replica.

The characteristics of the self-locked time gate are experimentally investigated. In the experiment, a 10 GHz 1.5 ps (FWHM) Gaussian shaped pulse train is used as an input, whose center wavelength is at 1550 nm. The input operating power (at point α) is 14 mW, which means that the required peak power is 0.86 W. A span of 2 km DFF is used for supercontinuum generation and a 2 nm BPF centered at 1545 nm is to filter out the clock signal. In the two branches, two attenuators (ATT) and two polarization controllers (PC) are placed before coupling to optimize the FWM condition. In the second stage, a semiconductor optical amplifier (SOA) or a span of 100 m highly nonlinear fiber (HNLF) is used as an NLE.

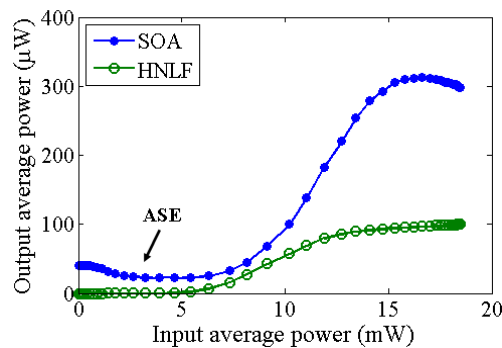


Fig. 3. Operation principle of the self-locked time gate.

The transfer function is illustrated in Fig. 3. The input average power (P_α) and output average power (P_β) are measured at the points α and β in Fig. 2. When input power is low, there is no output if the HNLF is used, while there are some very low outputs if the SOA is used, resulted from amplified spontaneous emission (ASE). When high power is input, high outputs can be obtained for both cases and the output power in the case of SOA is three times as that in the case of HNLF. Thus, the time gate can be applied to remove low-intensity noises, such as MAI. Insertion loss ($10\log(P_\beta/P_\alpha)$) of the time gate using the SOA and the HNLF are about -16 dB and -21 dB at the operating points. Besides, the time gate using the HNLF is more polarization-sensitive. Therefore, the time gate using the SOA is used in the further experiments.

4. Experimental demonstration and results

Figure 4 shows the experimental setup of a 4-user downlink and 4-user uplink OCDMA-PON. In the downlink, a train of Gaussian shaped optical pulses generated from a mode locked laser diode (MLLD) is modulated with a $2^{15}-1$ pseudorandom binary sequence (PRBS) by a PM and then split into four branches. On each branch, the modulated pulse train is encoded by a 640 Gchip/s $0/\pi$ -phase-shift SSFBG encoder. Four 31-chip Gold codes are

used. After power balance and decoherence, the encoded signals are coupled and transmitted to the ONU side through a span of single-mode fiber (SMF) and dispersion-compensation fiber (DCF) with a total length of 50 km. The waveform of 4-user multiplexing signals is shown in Fig. 5(a). In the ONU, the encoded signal is decoded and passed through the time gate. The waveforms of the decoded signals and the signals after the time gate are illustrated in Fig. 5(b)–5(i). After that, the signal is separated into two branches. In the upper branch, the signal is demodulated by a DPSK demodulator which is an asymmetric one-bit delay interferometer and detected by a balanced photodetector. The signal in the lower branch is for the uplink.

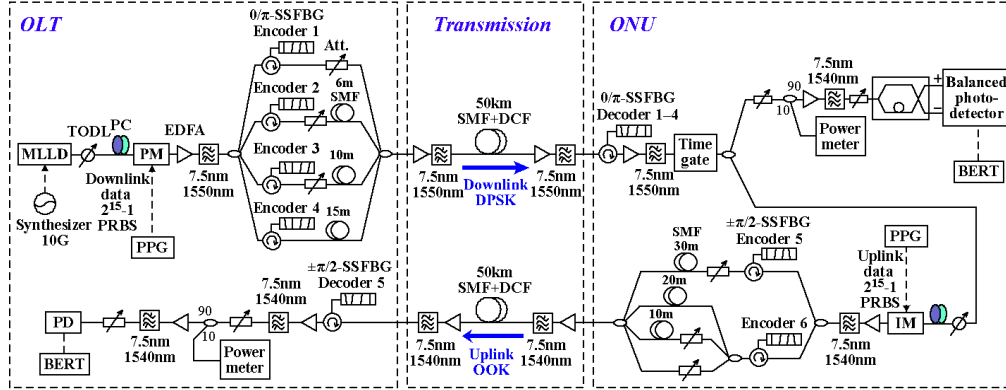


Fig. 4. Experimental setup of the duplex multi-user OCDMA system: a 50 km 4-user 10 Gbit/s/user DPSK downstream link and a 50 km 4-user 10 Gbit/s/user OOK upstream link.

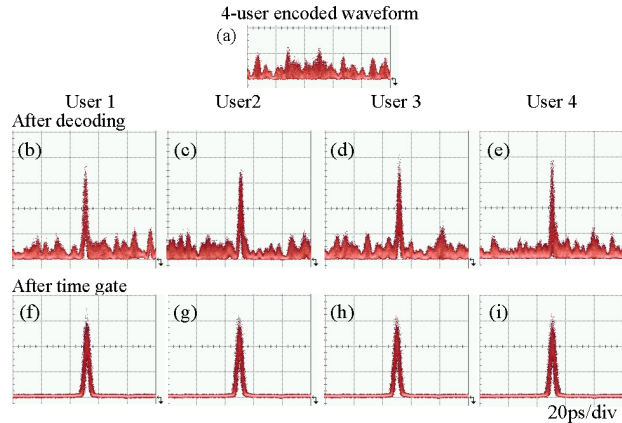


Fig. 5. Downlink waveforms of (a) 4-user multiplexing encoded signal, (b)–(e) signals after decoding, and (f)–(i) signals after time gate.

In the uplink, the signal is modulated by an IM. The clock recovery section is omitted in the experiment. The modulated signal is then split into two branches and encoded by two 31-chip 640 Gchip/s $\pm \pi/2$ -phase-shift SSFBG encoders [12]. The signal encoded by Encoder 6 is divided into three replicas to represent three MAI-users. After power balance and pattern decorrelation, the encoded signals are combined by a power coupler and transmitted to the OLT through a span of 50 km fiber (SMF + DCF), as shown in Fig. 6(a). In the OLT, the encoded upstream is decoded by Decoder 5 and detected by a photodetector. The decoded waveform is shown in Fig. 6(b).

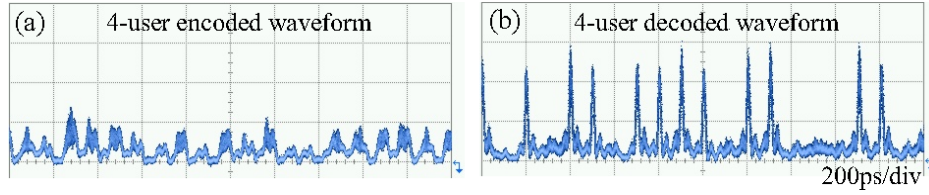


Fig. 6. Uplink waveforms of (a) 4-user multiplexing encoded signal and (b) signal after decoding.

Eye diagrams for both uplink and downlink are shown in Fig. 7, where clear open eyes can be observed. Compared with the eye diagram in Fig. 7(e)–7(h), the noises in Fig. 7(a)–7(d) are efficiently removed after the time gate. In the uplink, MAIs can be observed in the 4-user situation, as shown in Fig. 7(k), but the eyes are widely and clearly opened. BER performances with and without transmission are plotted in Fig. 8, where error-free ($\text{BER} < 10^{-9}$) measurements are achieved for all cases. The DPSK downlink has better performance than the OOK uplink, where the power penalty is about 2–5 dB. It is worth noting that there is a 3 dB difference between the DPSK and OOK receiver sensitivity. Thus, the degradation resulted from the remodulation is not serious.

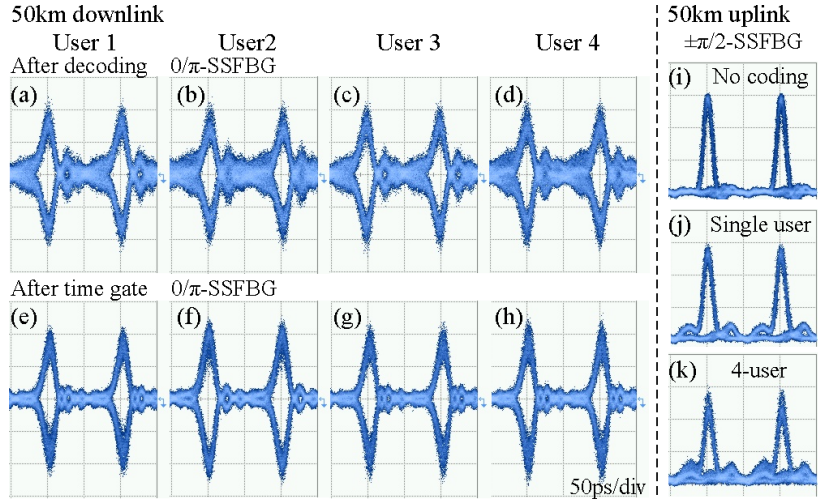


Fig. 7. Eye diagrams of (a)–(d) downstream signals after decoding, (e)–(h) downstream signals after time gate and (i)–(k) upstream signals without coding, for single user and 4-user.

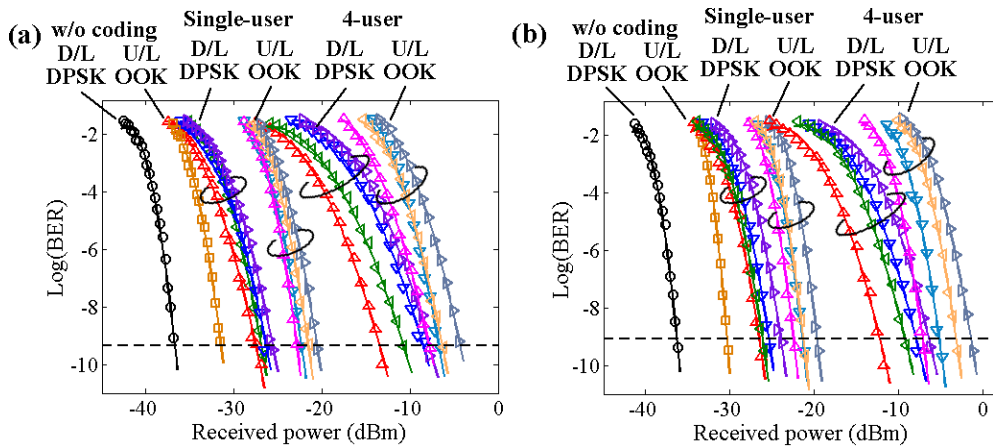


Fig. 8. BER performances in the situations of (a) back-to-back and (b) 50 km uplink and 50 km downlink.

The experimental demonstration is only to show the feasibility of the proposed OCDMA-PON. It has potential to further improve the system performance by applying a threshold or a time gate to remove MAIs in the uplink. Besides that, like some hybrid systems for next-generation PON stage 2 (NG-PON2) such as time/wavelength-division multiplexing (TWDM) systems [5, 23], large scalability of the network can be achieved by introducing WDM techniques into the OCDMA-PON [1].

5. Discussions

5.1 Performance improvement by employing all-optical self-clocked time gate

The all-optical self-clocked time gate is proposed and used in the OCDMA system for the first time. To acquire the potential properties of the time gate, the influence over the system improvement resulted from the time gate is experimentally investigated.

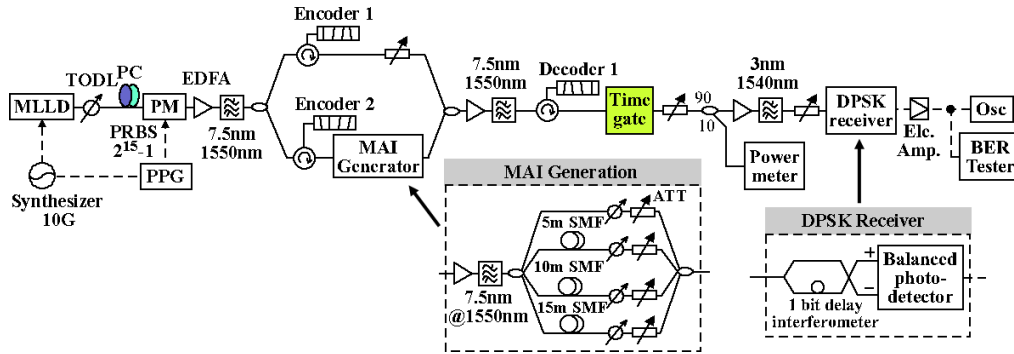


Fig. 9. Experimental setup of multi-user DPSK OCDMA system.

The performance analysis is carried out experimentally in the worst and the best situations which are defined as the most and the least MAIs overlapping with the target signal in the detection window. Figure 9 illustrates the measurement setup. A train of phase-modulated pulses are split into two branches and encoded by two encoders. In the measurement, not only 31-chip SSFBG en/decoders but also 63-chip 640 Gchip/s SSFBG en/decoders are tested. In the lower branch, the encoded pulse train is input into an MAI generator, which is to generate up to four MAIs by temporal pattern misalignment and power balance. Then, all encoded signals are multiplexed and transmitted to the receiving side. In the receiving side, the encoded signals are decoded and fed into the time gate. After the time gate, the signals are detected by a DPSK receiver, which consists of a one-bit delay interferometer and a balanced

photodetector. In the experiment, the worst and the best situations are realized by adjusting the temporal alignment of each MAI user. Figure 10 shows the power penalties between the situations with and without the use of the time gate. This comparison is conducted under the conditions when BER is 10^{-5} while the number of MAIs varies. The negative power penalty means the improvement of the performance while the positive values stands for the degradation. The worst and the best situations give upper and lower boundaries of the performance. The time gate cannot help the system to improve the performance when few MAIs overlap with the target signal, because in these situations the ASE noise from the SOA in the time gate dominates the degradation rather than the MAIs. When the number of MAIs increases, the time gate has more contributions to performance improvement, due to the efficient elimination of MAIs, which benefits multi-user systems.

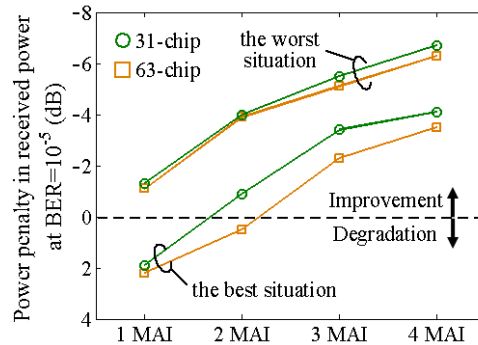


Fig. 10. Experimental measurement of system improvement by using the time gate.

5.2 Consideration of the power budget of the duplex transmission

In the proposed scheme, there are no light sources in the ONUs. To ensure the transmission quality, especially for the uplink transmission, power consumption in the each stage should be well planned. Thus, a power budget of the proposed duplex transmission system is evaluated. In the analysis of power budget, specific conditions, such as special characteristics of coding devices and optical codes, are not taken into the consideration and only power consumptions are used for calculation.

Table 1. Power contribution of each component

Item	Power in	Loss/Ga
Light source	0 dBm	
PM modulator		-5 dB
IM modulator		-5 dB
En/decoder		-15 dB
Transmission fiber		-0.2 dB/km
Multiplexing/Demultiplexing		L_c dB
Time gate		-16 dB
Erbium doped fiber amplifier (EDFA)		+ 14 dB
System margin	8 dB	
DPSK receiver sensitivity	-40 dBm	
OOK receiver sensitivity	-37 dBm	

Table 1 lists the power consumption of each component used in the duplex transmission. There are two factors affecting the power budget, the total number of users, K , and the transmission distance, L . The total number of users is related to multiplexing/demultiplexing loss, $L_c = -3 \lceil \log_2^K \rceil$ where $\lceil u \rceil$ denotes the smallest integer larger than or equal to u . A

power budget model is illustrated in Fig. 11. Components used in the duplex transmission are depicted in the model and their loss and gain are listed. In the analysis, the maximum transmission distance is investigated without in-line amplifications. Besides, an 8 dB system margin is considered in the both downlink and uplink for a high tolerance of deterioration in the transmission.

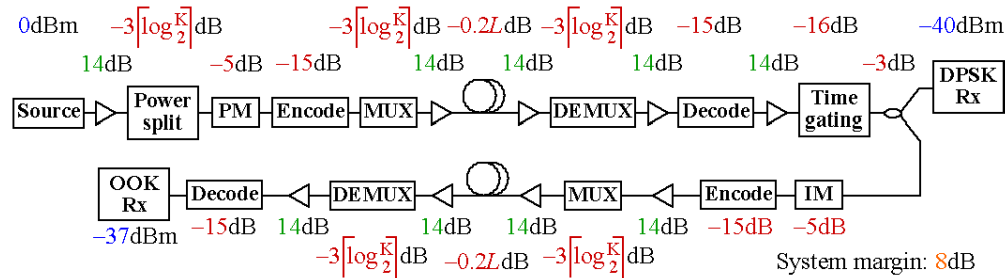


Fig. 11. Power budget model.

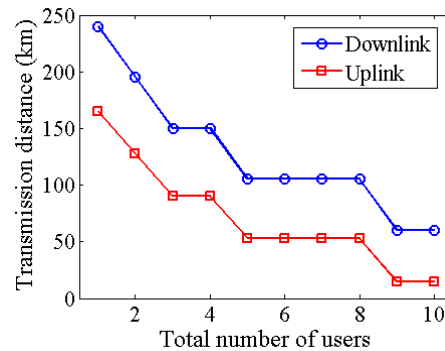


Fig. 12. Relationship between transmission distance and total number of users

According to the power budget model, the relationship between the transmission distance and the number of users for both downlink and uplink are calculated and depicted in Fig. 12. The transmission distance descends with the increase of the total number of users, which is mainly resulted from the coupling loss. Since the uplink experiences more power loss, the duplex transmission is mainly limited by the performance of the uplink. For a 50 km duplex transmission, the total number of users can be up to 8. Furthermore, employing en/decoders with low insertion-loss can significantly reduce the power consumption. For example, the proposed SSFBG en/decoders in [24] adopting apodization technique have insertion loss of only -1 dB. By using these kinds of en/decoders, there will be 28 dB and 56 dB improvements in the downlink and uplink respectively. The improved power efficiency ensures a higher signal-to-noise ratio (SNR) and a better system performance, which allows a longer transmission. To obtain a large number of users in the OCDMA system, optical codes with good aperiodic correlation should be used.

7. Conclusion

We have proposed and demonstrated an asynchronous 4-user 10 Gbit/s/user 50 km OCDMA-PON. The duplex transmission was based on remodulating DPSK downstream signals into OOK format for upstream transmission, which realized the centralized light source in the OLT and made ONUs source-free. Error-free transmissions have been achieved both in the uplink and downlink. Besides, we have investigated an all-optical self-locked time gate for signal regeneration. The time gate could efficiently extract the target signals by using self-generated clock signals, which provided the advantage of asynchronization to the transmission

system. With the help of the time gate, the downstream signal qualities were significantly improved, thus making it possible to remodulate the downstream signals for further upstream transmission. Furthermore, we have built a power budget model to evaluate the power consumption of the proposed OCDMA-PON. Due to the source-free ONUs, it was upstream transmission that limited the transmission distance, which was shortened by increasing the total number of users. To enhance the energy efficiency and extend the transmission distance, en/decoders with low insertion-loss were suggested to be employed. The proposed OCDMA-PON is a promising candidate for future miscellaneous networks and the related techniques have potential to be applied to other secure transmission systems.

Acknowledgment

The authors would like to thank Dr. J. M. Delgado Mendinueta for a fruitful discussion and Mr. H. Sumimoto of NICT for his technical support. Bo appreciates the Internship Research Fellowship awarded by NICT.